Development 139, 215-224 (2012) doi:10.1242/dev.063875

Engrailed homeoprotein recruits the adenosine A1 receptor to potentiate ephrin A5 function in retinal growth cones

Olivier Stettler[1,2], Rajiv L. Joshi[1,3], Andrea Wizenmann[4], Jürgen Reingruber[3,5], David Holcman[3,5], Colette Bouillot[1,3], François Castagner[1,3], Alain Prochiantz[1,3,6,*] and Kenneth L. Moya[1,3,*]

SUMMARY

Engrailed 1 and engrailed 2 homeoprotein transcription factors (collectively Engrailed) display graded expression in the chick optic tectum where they participate in retino-tectal patterning. In vitro, extracellular Engrailed guides retinal ganglion cell (RGC) axons and synergises with ephrin A5 to provoke the collapse of temporal growth cones. In vivo disruption of endogenous extracellular Engrailed leads to misrouting of RGC axons. Here we characterise the signalling pathway of extracellular Engrailed. Our results show that Engrailed/ephrin A5 synergy in growth cone collapse involves adenosine A1 receptor activation after Engrailed-dependent ATP synthesis, followed by ATP secretion and hydrolysis to adenosine. This is, to our knowledge, the first evidence for a role of the adenosine A1 receptor in axon guidance. Based on these results, together with higher expression of the adenosine A1 receptor in temporal than nasal growth cones, we propose a computational model that illustrates how the interaction between Engrailed, ephrin A5 and adenosine could increase the precision of the retinal projection map.

KEY WORDS: ATP, Engrailed, Ephrin, Adenosine, Axon guidance, Homeoprotein, Chick, Mouse

INTRODUCTION

Information processing in the brain depends on precise neuronal connections established during development and involves axon guidance molecules that repel advancing growth cones from inappropriate areas and/or attract growth cones to appropriate target areas (Flanagan, 2006; Scicolone et al., 2009). In the primary visual projection, retinal ganglion cell (RGC) axons from the nasal retina project to the posterior optic tectum and axons from the temporal retina project to the anterior tectum so that the temporal-nasal (T-N) axis of the retina maps along the anterior-posterior (A-P) axis of the tectum/superior colliculus. The low-to-high A-P repulsion of axons from temporal retina is due, in part, to EphA forward signalling controlled by a diminishing T-N gradient of EphA receptors on RGC axons and an increasing gradient of Ephrin-As in the tectum (Flanagan, 2006; Scicolone et al., 2009).

Engrailed 1 and engrailed 2 (collectively Engrailed, or En) homeodomain transcription factors regulate Ephrin expression in a cell-autonomous manner in the chick optic tectum (Logan et al., 1996). However, Engrailed, as with many homeoproteins, transfers between cells and has non-cell-autonomous activities in gene transcription and protein translation (Brunet et al., 2007; Joliot and Prochiantz, 2004; Prochiantz and Joliot, 2003). In vitro, exogenous Engrailed attracts RGC axons from nasal *Xenopus* retina and repels axons from RGCs in temporal retina (Brunet et al., 2005). The guidance activity of Engrailed in *Xenopus* RGC growth cones requires the internalisation of the protein and is blocked by inhibitors of protein translation (Brunet et al., 2005). Furthermore, Engrailed exerts guidance activity when the growth cone is isolated from the soma, indicating that it acts locally. In the chick optic tectum, extracellular Engrailed is present in a low-to-high A-P gradient in the tectum and blocking extracellular Engrailed in this region leads to misrouting of RGC axons (Wizenmann et al., 2009). In chick retinal explants, exogenous Engrailed sensitizes the growth cones of axons of temporal RGCs to ephrin A5 collapsing activity through a mechanism that requires Engrailed-dependent protein translation (Wizenmann et al., 2009).

Here, we characterise the molecular mechanism by which exogenous Engrailed potentiates ephrin A5-induced growth cone collapse. We find that Engrailed stimulates rapid ATP synthesis and secretion from growth cones. Inhibiting extracellular ATP hydrolysis blocks the Engrailed/Ephrin synergy in growth cone collapse, whereas increasing ATP hydrolysis enhances it. Engrailed/ATP enhancement of growth cone collapse occurs via activation of the adenosine A1 receptor (A1R), which is present at higher concentrations in temporal than nasal growth cones. These data were used to construct a computational model that describes how the physiological interaction between Engrailed, ephrin A5 and adenosine may enhance retino-tectal map precision. Our results provide new insight into the non-cell-autonomous activity of homeoproteins.

MATERIALS AND METHODS

Reagents and proteins

All reagents were purchased from Sigma unless otherwise specified. En1 and En2 (collectively En) have similar effects on axon guidance (Brunet et al., 2005; Friedman and O'Leary, 1996; Itasaki and Nakamura, 1996; Wizenmann et al., 2009) and were used with identical results. Engrailed proteins were produced in *E. coli* and purified using published procedures (Brunet et al., 2005).

[1]CNRS Unité mixte de Recherche 7241/INSERM U1050. Equipe FRM, Center for Interdisciplinary Research in Biology (CIRB), Collège de France, 11, place Marcelin Berthelot, 75005 Paris, France. [2]CNRS Unité mixte de Recherche 8192, Laboratoire de dynamique membranaire et maladies Neurologiques, Université Paris Descartes, Sorbonne Paris Cité, 45 rue des St-Pères, 75005 Paris, France. [3]Labex Memolife, Paris Sciences Lettres Research University, Ecole Normale Supérieure, 45 rue d'Ulm, 75005 Paris, France. [4]Institute of Anatomy, University of Tübingen, Österbergstrasse 3, 72074 Tübingen, Germany. [5]Institut de Biologie, Ecole Normale Supérieure (CNRS/INSERM), 46 rue d'Ulm, 75005 Paris, France. [6]Ecole Doctorale 158, University Pierre et Marie Curie, Bâtiment B, 7ème étage Case 25, 9 Quai Saint Bernard, 75007 Paris, France.

*Authors for correspondence (alain.prochiantz@college-de-france.fr;ken.moya@college-de-france.fr)

Accepted 27 October 2011

Proteomic analysis and ATP measurement from the growth cone fraction

Growth cones were prepared from embryonic day (E) 17 mouse superior colliculus as described (Gordon-Weeks and Lockerbie, 1984). Briefly, tissue samples were homogenised in sucrose/Hepes buffer, centrifuged at 13,000 ***g*** and the pellets homogenised and separated on a 7% Ficoll/0.32 M sucrose gradient at 42,000 ***g***. Growth cones were recovered in 600 μl incubation buffer (10 mM Tris pH 7.4, 2.2 mM $CaCl_2$, 0.5 mM Na_2HPO_4, 0.4 mM KH_2PO_4, 4 mM $NaHCO_3$, 6.25 mM NaCl) and incubated at 37°C for 10 minutes. [^{35}S]-labelled amino acids (107 μCi, Promix; GE Healthcare Life Sciences) diluted in 120 μl incubation buffer at 37°C for 10 minutes were added to the growth cones and the mixture was separated into four aliquots. En (3 μg) dissolved in 300 μl Hanks' balanced salt solution (HBSS) was added (140 nM final concentration) to two of the aliquots and two aliquots received HBSS alone. After incubation for 1 hour at 37°C, the samples were centrifuged at 13,000 ***g*** at 4°C for 20 minutes. Supernatants were discarded and the growth cone pellets immediately frozen on dry ice.

The growth cone pellets were solubilized in running buffer [8 M urea, 4% (w/v) CHAPS, 20 mM DTT, 0.2% ampholines (BioLytes 3-10, BioRad)] and subject to isoelectrofocusing (IEF; Ready Strip IPG Strip 11 cm pH 3-10, BioRad) at 50,000 Vh. IEF strips were equilibrated for 15 minutes in Equilibration buffer I (6 M urea, 2% SDS, 0.375 M Tris-HCl pH 8.3, 20% glycerol, 130 mM DTT) and for 20 minutes in Equilibration buffer II (as Equilibration buffer I but with 135 mM iodoacetamide in place of DTT). IPG strips were placed on a 7-15% gradient SDS-PAGE gel and proteins separated in the second dimension and then transferred onto PVDF filters (Immobilon, Millipore). PVDF filters were placed against BioMax MB film (Kodak) for 54 days. The autoradiograms were used as a template to excise labelled protein spots from the PVDF filter. The protein spots were then analysed by liquid chromatography electrospray ionization tandem mass spectroscopy (LC-ESI-MS/MS).

For ATP measurement, growth cones were harvested in Krebs buffer and stimulated for 1 or 5 minutes at 37°C with Engrailed (4.6 μM). The growth cones were chilled on ice, centrifuged at 13,000 ***g*** for 10 minutes at 4°C and the supernatant transferred to a new tube. ATP was detected in the growth cone-containing pellet fraction and in the supernatant using a standard luminescence assay (ATP Lite, PerkinElmer).

Embryonic chick retinal explants, western blotting and growth cone collapse assay

Six-well plates or coverslips in 24-well plates were coated with poly-D-lysine (0.1 mg/ml) overnight and then with laminin (10 μg/ml in PBS) for 3-4 hours at 37°C. Eyes from E6 chick embryos were placed in HBSS and the lens and vitreous removed. Using the ventral streak as a landmark, a wedge containing the temporal edge (or the nasal edge) of the retina was removed and flattened. Strips of extreme temporal or nasal retina 200-300 μm wide were cut into squares and transferred to culture wells containing 500 ml MSS [0.075% (w/v) HCO_3, 10 mM Hepes pH 7.4, 2 mM glutamine, 0.6% (w/v) glucose] culture medium supplemented with 10% foetal bovine serum (FBS).

For Ndufs3 western blotting, E6 chick retinae were dissociated and cultured in MSS/FBS for 3 days. The cultures were treated for 30 minutes with 12 nM Engrailed and the cells recovered in 50 mM Tris-HCl pH 8, 150 mM NaCl and 1% (v/v) Nonidet P40. Protein concentration was determined using the 660 nm Protein Assay Reagent (Pierce) and 4 μg of protein were separated by SDS-PAGE and transferred to ImmobilonP membranes. Ndufs3 was detected using anti-Ndufs3 antibody (1:2000, Abcam) and chemiluminescence with ECL Plus reagent (GE Healthcare). Images were acquired with an LAS 400 imager (Fuji). Band intensities were quantified using ImageJ (NIH) and corrected using actin as a sample loading control. Data are the average of two western blots of three different wells for each condition.

Cell cultures (48 hours old) were used both for ATP imaging and for the collapse assay (see below). The following proteins/drugs were used for the collapse assay: En (75 nM), apyrase (10 U/ml), anisomycin (25 μM), α,β- and β,γ-methylene-ATP (300 μM each), CGS15943 (1 μM), DPCPX (100 nM), ZM 241385 (500 nM) and CCPA (1 μM).

Extracellular ATP imaging

Extracellular ATP was measured from RGC growth cones by fluorescence microscopy (Corriden et al., 2007). The assay is based on the conversion of non-fluorescent oxidised NADP added to the medium to its fluorescent and reduced counterpart NADPH in an equimolar ratio in the presence of ATP. The conversion is driven by the addition, just before imaging, of hexokinase (2.7 U/ml) and glucose 6-phosphate dehydrogenase (3 U/ml) in the presence of NADP (2.4 mM) and glucose (12 mM). Images were acquired using a Cool Snap ES camera (Nikon; 700 msecond exposure time) mounted with a Nikon oil-immersion objective (×100). Microscope filters optimised NADPH fluorescence detection (340 nm bandpass excitation, 450 nm bandpass emission). ImageJ software was used to extract fluorescence intensity values. A threshold level of fluorescence intensity was chosen (for all images) in ImageJ in order to suppress artifactual background fluorescence. Integrated densities measured at the level of the growth cone were normalised to background intensity and to growth cone area. We verified that the addition of the mixture did not stimulate ATP release. Other controls without NADP and enzymes in the substrate mixture but in the presence of glucose and Engrailed were performed to verify that cell stimulation by the homeoprotein did not alter autofluorescence levels. Finally, growth cones that underwent massive morphological changes during recording were excluded from the analysis.

Engrailed (K313E)

Translation-deficient engrailed 1 mutated at position 313 will be described and characterised elsewhere. Briefly, the eIF4E-binding site of mouse En1 was targeted by a mutation of lysine 313 to a glutamic acid residue. The mutant protein failed to bind eIF4E (GST pull-down experiments) and to induce Ndufs3 protein synthesis in mouse midbrain cultures.

Immunofluorescence

A1R antibodies (Abcam ab3460 or Santa Cruz sc28995) were used at 1:100 in PBS containing 0.2% Triton X-100 (PBST)/1% FBS after an initial blocking step in PBST/10% FBS. To quantify A1R immunofluorescence, images were converted to black and white and the lookup table changed in ImageJ. The background signal was the same in images of nasal and temporal explants. The threshold function of ImageJ was used to delimit the contour of growth cones. The integrated density for each growth cone was measured and then normalised to the growth cone area.

Stripe assay

Chick axon guidance experiments on stripes of tectal membranes were performed as described (Wizenmann et al., 2009). Briefly, membranes from the anterior and posterior thirds of E9 tecta were progressively aspirated into 90 μm stripes on Nuclepore filters (0.1 μm). DiAsp-labelled (10 μl of 5 mg/ml stock per 2 ml HBBS) retina strips were adjusted orthogonally onto the membrane stripes and fixed with metal weights and cultured for 2 days (in F12:DMEM with 10% FBS) before fixing. The cultures were mounted in 1% DABCO in 10:1 glycerol: PBS before observation under a fluorescence microscope. To generate a quantitative index of RGC axon growth on membrane stripes, the integrated fluorescent signal from the axons in the stripe versus total integrated axon fluorescence was calculated for a rectangular region of interest that spanned the width of the image adjacent to the explant edge.

A computational model for the synergistic effect between Engrailed and ephrin A5 signalling on growth cone collapse

Following previous theoretical and experimental studies, we represented a graded distribution of EphA2 in the retina and of ephrin A5 and extracellular Engrailed in the tectum (Baier and Bonhoeffer, 1992; Brown et al., 2000; Goodhill and Baier, 1998; Holcman et al., 2007; Reber et al., 2004; Wizenmann et al., 2009; Yates et al., 2004; Yates et al., 2001) by an exponential function. Based on the differential density of A1R on nasal and temporal axons, we further assumed a graded expression of A1R in growth cones depending on the initial axon position in the retina. All concentration profiles are approximated as exponentials.

We scaled parameters by the lengths in the retina and tectum so that coordinates x=0 and x=1 corresponded to the most nasal and temporal positions in the retina, respectively, and coordinates y=0 and y=1 to the most anterior and posterior positions in the tectum, respectively. The ephrin A5, EphA2, Engrailed and A1R gradients in the retina and the tectum are given by equations:

$$E(x) = E_{min}e^{\beta_E x}, \quad e(y) = e_{min}e^{\beta_e y}, \\ eg(y) = eg_{min}e^{\beta_{eg} y}, \quad A(x) = A_{min}e^{\beta_A x}, \tag{1}$$

where β_E, β_e, β_{eg} and β_A characterise the steepness of the gradients.

In our model, a growth cone originating at retinal position x perceives at tectal position y an ephrin A5 signal $S_e(x,y)$ that is proportional to the EphA2 concentration on the growth cone and to the ephrin A5 concentration in the tectum, and an Engrailed signal $S_{eg}(x,y)$ that is proportional to the Engrailed and A1R concentrations. We used the expressions:

$$S_e(x,y) = \alpha_e E_r(x) e_t(y) = \alpha_e E_{r,min} e_{t,min} e^{\beta_E x + \beta_e y}, \tag{2}$$

$$S_{eg}(x,y) = \alpha_{eg} A(x) eg(y) = \alpha_{eg} A_{min} eg_{min} e^{\beta_A x + \beta_{eg} y}, \tag{3}$$

where α_e and α_{eg} are constants.

Axonal stopping position in the tectum without Engrailed feedback

In the absence of Engrailed feedback, we assumed that a growth cone originating at retinal position x and moving along the A-P axis of the tectum collapses (and stops) when the ephrin A5 signal $S_e(x,y)$ reaches a given threshold T. By $T=e^{\kappa}\alpha_e E_{r,min} e_{t,min}$ (the parameter $\kappa>1$ modulates the threshold value) and by solving the equation $S_e(x,y)=T$, we found that the axonal mapping from the retina to the tectum is linear, as is observed experimentally (e.g. Reber and Lemke, 2005), and described by:

$$y = \frac{\kappa}{\beta_e} - \frac{\beta_E}{\beta_e} x. \tag{4}$$

To account for variability, we assumed that a growth cone originating at retinal position x_0 collapses when the ephrin A5 signal $S_e(x_0,y)$ is within the range $(T-\delta T, T+\delta T)$. Accordingly, its final tectal position (stop position) fluctuates in the interval:

$$\left(y_0 - \frac{\delta_{y_0}}{2}, y_0 + \frac{\delta_{y_0}}{2}\right),$$

where y_0 is determined from $S_e(x_0,y_0)=T$. In first order in $\delta T/T$ the fluctuation in the position is given by:

$$\delta y_0 = \frac{2}{\beta_e}\frac{\delta T}{T}. \tag{5}$$

Axonal stopping position in the tectum with Engrailed feedback

Based on our experimental findings, we now propose a new scenario where Engrailed non-linearly amplifies the ephrin A5 signal once the Engrailed signal S_{eg} reaches a certain strength T_{eg}. For the amplified ephrin A5 signal $\tilde{S}_e(x,y)$ we propose the expression:

$$\tilde{S}_e(x,y) = S_e(x,y)\left(1 + \Lambda\left(\frac{S_{eg}(x,y)}{T_{eg}}\right)\right), \tag{6}$$

where $\Lambda(s)$ is a sigmoid function with:

$$\Lambda(s) = 0, \text{ for } s \approx 0 \text{ and } \Lambda(s) = \alpha, \text{ for } s \approx 1. \tag{7}$$

In practice, $\Lambda(s)$ has to be determined from the molecular interactions. In the absence of precise knowledge concerning these interactions, we approximated $\Lambda(s)$ by the sigmoid function $\Lambda(s)=\alpha(1+\tanh((s-1)/0.1))/2$ (Fig. 1).

A growth cone originating from retinal position x_0 collapses when experiencing an Engrailed-amplified ephrin A5 signal $\tilde{S}_e(x_0,y)$ in the range $(\tilde{T}-\delta\tilde{T}, \tilde{T}+\delta\tilde{T})$, leading to a stop position in the range:

$$\left(\tilde{y}_0 - \frac{\delta_{\tilde{y}_0}}{2}, \tilde{y}_0 + \frac{\delta_{\tilde{y}_0}}{2}\right).$$

We assume that the threshold $\tilde{T}$ is also Engrailed amplified and is larger than with T. When $\beta_{eg}/\beta_A=\beta_e/\beta_E$ is satisfied we have $S_{eg}(x_0,y_0)=\zeta S_e(x_0,y_0)=\zeta T$, where ζ is a constant. Furthermore, by choosing $T_{eg}=\zeta T$ and $\tilde{T}=T(1+\Lambda(1))$ we found that the stop condition $\tilde{S}_e(x_0,\tilde{y}_0)=\tilde{T}$ leads to $\tilde{y}_0=y_0$; thus, we obtained the same mapping as in absence of Engrailed. For the variance $\delta\tilde{y}_0$ we obtain in first order of $\delta\tilde{T}/\tilde{T}$ the expression:

$$\delta\tilde{y}_0 \approx \frac{2}{\beta_e + \beta_{eg}\frac{\Lambda'(1)}{1+\Lambda(1)}}\frac{\delta\tilde{T}}{\tilde{T}} = \frac{1}{1+\frac{\beta_{eg}}{\beta_e}\frac{\Lambda'(1)}{1+\Lambda(1)}}\delta y_0 << \delta y_0, \tag{8}$$

where we used $\delta T/T=\delta\tilde{T}/\tilde{T}$ and inserted δy_0 from equation 5. Interestingly, when $\beta_{eg}/\beta_A=\beta_e/\beta_E$, Engrailed increases the axonal stop precision, but does not change the retina-to-tectum mapping defined by ephrin A5 signalling ($\tilde{y}_0=y_0$). By contrast, when $\beta_{eg}/\beta_A\neq\beta_e/\beta_E$, in order to achieve $\tilde{y}_0=y_0$, the threshold T_{eg} would have to depend on x_0 and thus would need to be different between axons (a situation not examined here).

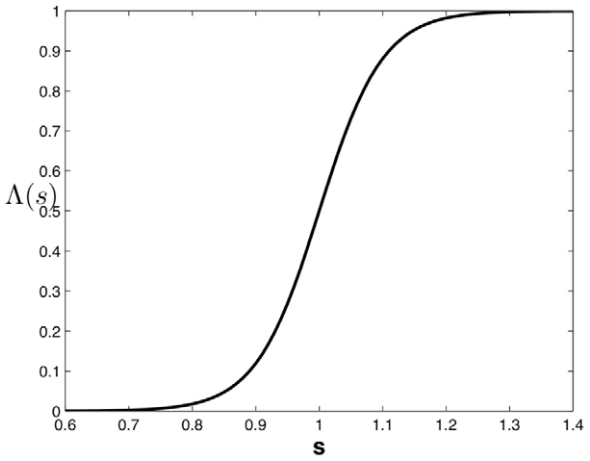

Fig. 1. Sigmoid function Λ(*s*) by which Engrailed amplifies ephrin A5 signalling. We use $\Lambda(s)=\alpha(1+\tanh((s-1)/0.1))/2$ with α=1.

RESULTS

Engrailed internalisation triggers ATP synthesis and release

We identified Engrailed translational targets by protein synthesis in E17 mouse dorsal mesencephalon fractions enriched in retinal growth cones. Metabolic labelling and 2D autoradiography showed a number of newly synthesized proteins, with some spots greatly increased after Engrailed stimulation (Fig. 2A,B). Mass spectroscopy identified a protein whose synthesis upregulated 8-fold by Engrailed as Ndufs3, a component of complex I of the mitochondrial respiratory chain. As is the case for the majority of mitochondrial proteins, the *Ndufs3* mRNA is transcribed in the nucleus, specifically targeted to mitochondria and translated locally in the cytoplasm prior to protein translocation into the organelle (Chihara et al., 2007).

We hypothesised that the translation of complex I Ndufs3 after Engrailed capture by growth cones could be associated with ATP production. To test this we measured ATP in the pellet and supernatant of the growth cone fraction prepared from E17 dorsal mouse mesencephalon. Engrailed stimulated a slight but significant increase in ATP in the growth cone pellet fraction at 5 minutes (Fig. 2C). Strikingly, Engrailed stimulated a greater than 5-fold increase in ATP in the supernatant. The changes in ATP in the pellet and supernatant were both blocked in the presence of the ATP synthase inhibitor oligomycin (Fig. 2C). These results show that Engrailed stimulates ATP synthesis and that most of the newly synthesized ATP is in the supernatant of the mouse growth cone preparation and thus extracellular. A significant increase in extracellular ATP was observed as early as 1 minute after Engrailed stimulation (supplementary material Fig. S1).

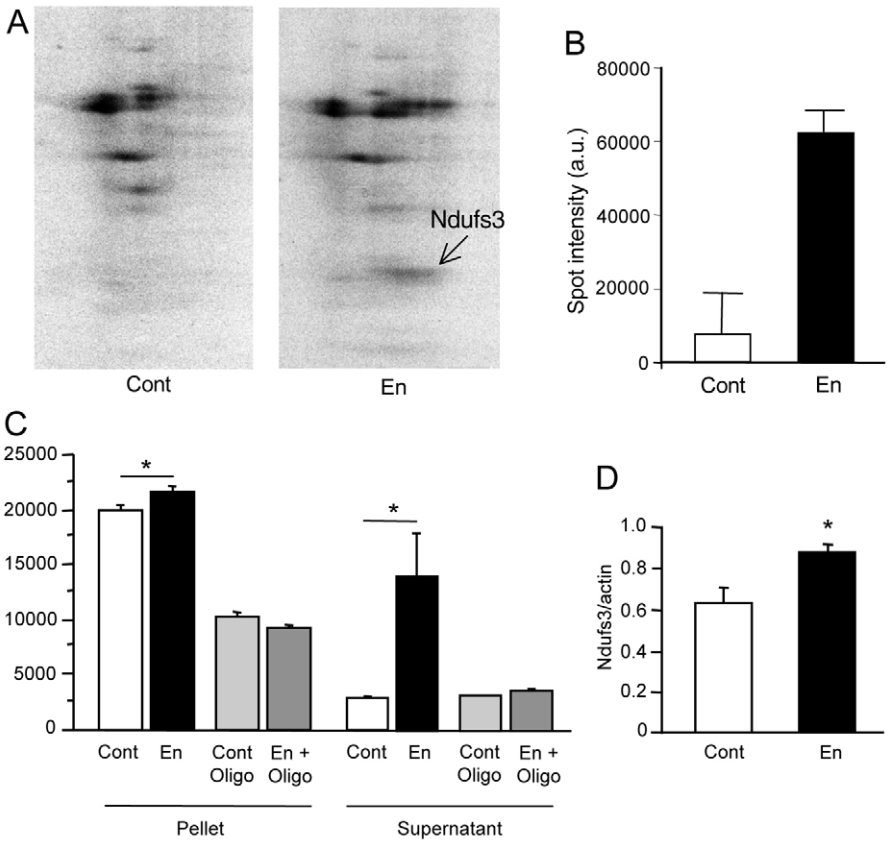

Fig. 2. Engrailed stimulates protein translation and ATP release.
(**A**) Autoradiogram of proteins separated by 2D electrophoresis after metabolic labelling of mouse E17 dorsal tectum growth cone preparation treated with vehicle (Cont) or Engrailed (En). (**B**) Densitometric analysis of the radioactive spot indicated by the arrow in A shows a large increase in neosynthesis in Engrailed-treated growth cones. This protein spot was identified by mass spectrometry as the nuclear-encoded mitochondrial protein Ndufs3. Mean ± s.d. of two preparations. (**C**) Engrailed stimulates ATP synthesis and release from E17 tectal growth cones. This increase is blocked in the presence of the ATP synthase inhibitor oligomycin. Mean ± s.e.m. of five separate samples treated in parallel. Statistical analyses were performed using one-way ANOVA ($P<0.001$) and two-tailed Student's *t*-test (*$P<0.05$). (**D**) Engrailed stimulates an increase in Ndufs3 western blot signal in dissociated embryonic chick retinal cells. *$P<0.05$, unpaired *t*-test. Mean ± s.e.m. from three separate culture wells.

Engrailed-induced collapse requires ATP formation

To examine whether ATP formation has a role in Engrailed-induced collapse (Wizenmann et al., 2009) we turned to E6 chick retinal explants in culture. We first established that Engrailed increases Ndufs3 expression in cultures of chick retinal cells. Ndufs3 was significantly increased, by about one-third, after 30 minutes of treatment with Engrailed (Fig. 2D). We then examined whether Engrailed leads to an increase in extracellular ATP also in this assay system. Using NADPH fluorescence to visualise and quantify extracellular ATP (Corriden et al., 2007), we observed increased fluorescence at the growth cone level within 1-5 minutes (average time of onset: 2 minutes 43 seconds) after the addition of Engrailed to the culture medium (Fig. 3A,B). This ATP response varied in initiation time, duration and intensity from growth cone to growth cone (Fig. 3C). Aligning the initiation times for the ten growth cones in Fig. 3C and averaging their responses results in a bell-shaped curve that peaks 100 seconds after the onset of ATP release (Fig. 3D). ATP release was blocked by pre-adsorbing Engrailed with an anti-Engrailed antibody, but not with an anti-Pax6 antibody (Fig. 3B,E,F), confirming that Engrailed is the active entity in the preparation.

Addition of the protein synthesis inhibitor anisomycin 10 or 45 minutes before Engrailed strongly inhibited the response (80% and 100% inhibition, respectively) without visible effects on growth cone morphology (Fig. 3G-J). Since the protein synthesis inhibitors anisomycin and cycloheximide can influence ATP turnover (Talha and Harel, 1986), we also used a translation-deficient mutant, En1 (K313E), to study the protein translation dependence of Engrailed effects (see Materials and methods). Extracellular ATP after En1 (K313E) addition was reduced by ~80% compared with wild-type Engrailed (Fig. 3G). Taken together, this series of experiments demonstrates that the addition of Engrailed induces a rapid and protein translation-dependent ATP synthesis and release by RGC growth cones.

The role of Engrailed-induced ATP release in growth cone behaviour was tested in the collapse assay. Fig. 4A illustrates the morphologies of control (left) and collapsed (right) temporal cones and Fig. 4B quantifies the collapsing activities in different conditions. Ephrin A5 at 0.1 μg/ml increases collapse frequency from 8 to 24%, as compared with the maximal 50% value obtained with 0.4 μg/ml. Engrailed alone at 75 nM has no effect but raises the frequency of growth cone collapse to 41% in the presence of 0.1 μg/ml ephrin A5. The protein synthesis inhibitor anisomycin only blocked the latter Engrailed synergizing activity, confirming that ephrin A5-induced collapse is not protein synthesis dependent, in contrast to the Engrailed activity (Wizenmann et al., 2009).

Ephrin A5/Engrailed synergy requires A1R purinergic signalling

To test whether Engrailed-induced ATP release is involved in the ephrin A5/Engrailed synergy, the ATP-degrading enzyme apyrase (Kettlun et al., 1982) was added to the bath. Apyrase had no effect of its own but further enhanced, up to 56%, the percentage collapse observed in the presence of both Engrailed and ephrin A5. Neither Engrailed nor ephrin A5 alone, or together, induced growth cone collapse in explants from E6 nasal retina (Fig. 4C) and the addition of apyrase had a small effect per se (a less than 2-fold increase, as compared with the 8-fold increase seen in temporal growth cones).

These results confirm the synergistic activity of Engrailed on ephrin A5 collapse and demonstrate that this synergy is protein synthesis dependent and higher on temporal than on nasal growth

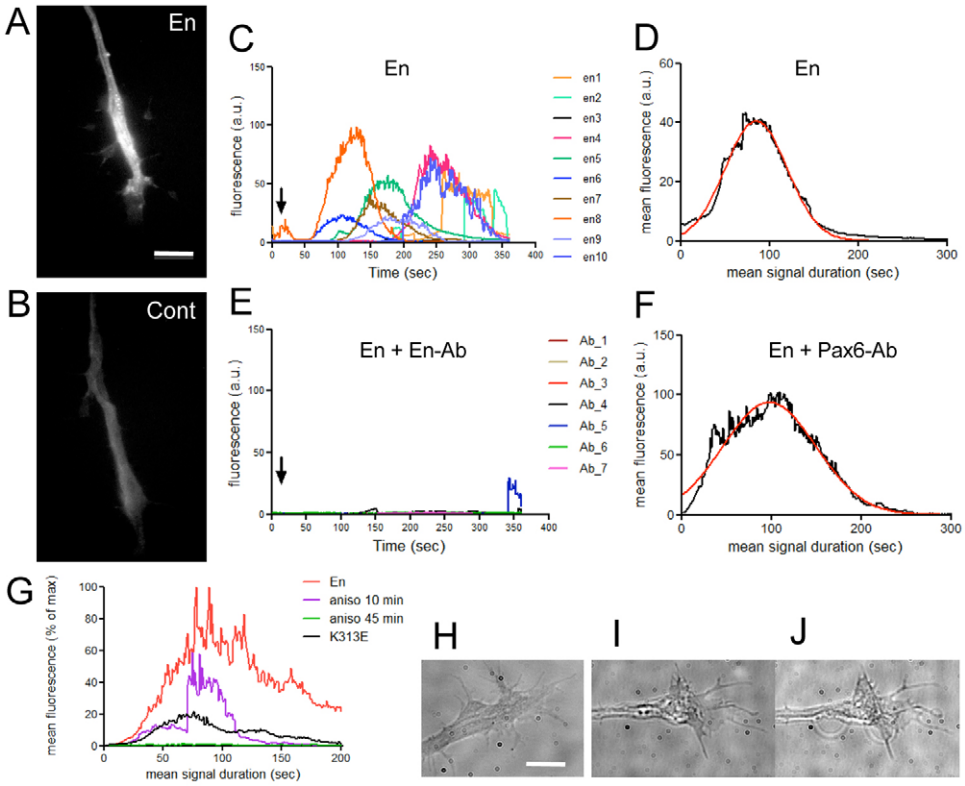

Fig. 3. Engrailed-induced ATP secretion from chick temporal growth cones. (**A**,**B**) NADPH fluorescence due to the presence of extracellular ATP of a growth cone treated with Engrailed (A) or a control treated with Engrailed preadsorbed with a blocking antibody (B) at peak signal intensity. (**C**) NADPH fluorescence over time for ten individual temporal growth cones. (**D**) Mean duration and intensity of the extracellular ATP signal after synchronization of traces shown in C. (**E**) Little or no NADPH fluorescence is recorded when growth cones are exposed to Engrailed pre-incubated with a specific anti-En antibody. (**F**) Pre-incubation of Engrailed with anti-Pax6 antibody does not significantly change NADPH fluorescence parameters. (**G**) Anisomycin decreases (10-minute preincubation) or abolishes (45-minute preincubation) Engrailed-induced ATP secretion. Engrailed (K313E), a mutant form with reduced protein translation activity, does not provoke full ATP release. (**H-J**) Normal cytoarchitecture of growth cones is maintained after 45 minutes of anisomycin plus Engrailed pre-treatment. A growth cone treated with En and anisomycin is shown before (I) and after (J) recording; control (H). Scale bars: 9 μm in A for A,B; 6 μm in H for H-J.

cones. The role of ATP synthesis and release remains open, as the ATP-degrading enzyme does not abolish, but rather enhances, the collapsing activity of the two factors added together.

A possible explanation for the latter result is that ATP degradation products, rather than ATP itself, participate in the Engrailed enhancing activity. We thus blocked ATP degradation with either α,β-methylene-ATP or β,γ-methylene-ATP, two ectonucleotidase inhibitors (Matsuoka and Ohkubo, 2004). These treatments abolished Engrailed synergistic activity (Fig. 4D), demonstrating that ATP is not the direct active compound but a source of active compounds. Furthermore, because α,β-methylene-ATP and β,γ-methylene-ATP are potent P2 and P2X receptor agonists, respectively (Burnstock, 2006; Burnstock, 2008), we could also rule out the possibility that ATP signals through these purinergic receptors to stimulate growth cone collapse.

RGCs express adenosine A1, A2A and A3 receptors (Kvanta et al., 1997). Therefore, among the possibly active ATP metabolites, we focused on adenosine. The broad-spectrum adenosine receptor antagonist CGS15943 significantly reduced Engrailed/ephrin A5-stimulated collapse and this effect was reproduced with DPCPX, an A1R-specific antagonist, but not with the A2A receptor antagonist ZM241385 (Ongini et al., 1999) (Fig. 4E). These results demonstrate that the effects of Engrailed on temporal growth cones are mediated by A1R activation.

A parsimonious hypothesis is that Engrailed induces ATP synthesis and release and that the degradation of ATP into adenosine leads to A1R activation, thus enhancing ephrin A5 activity. If this hypothesis is correct, a specific A1R agonist should have no effect of its own on collapse but should enhance ephrin A5 signalling in the absence of Engrailed. In agreement with this prediction, CCPA, a selective A1R agonist (Burnstock, 2006), alone (supplementary material Fig. S2) or with Engrailed (Fig. 4F), did not induce growth cone collapse in explants from temporal retina but could substitute for Engrailed in enhancing ephrin A5 activity (Fig. 4F).

If A1R stimulation is in the Engrailed signalling pathway, then the poor collapse response of nasal growth cones might in part reflect a difference in A1R density between nasal and temporal growth cones. In agreement with this hypothesis, A1R immunostaining is significantly more intense in the distal portions of temporal axons, including the growth cone, compared with nasal axons (Fig. 5A-C).

A1R purinergic signalling participates in temporal growth cone guidance

To directly test a role for A1R in axon guidance we used the stripe assay (Wizenmann et al., 2009). Strips of temporal retina were placed orthogonal to alternating stripes of anterior and posterior tectal membranes. Temporal axons labelled with DiAsp are

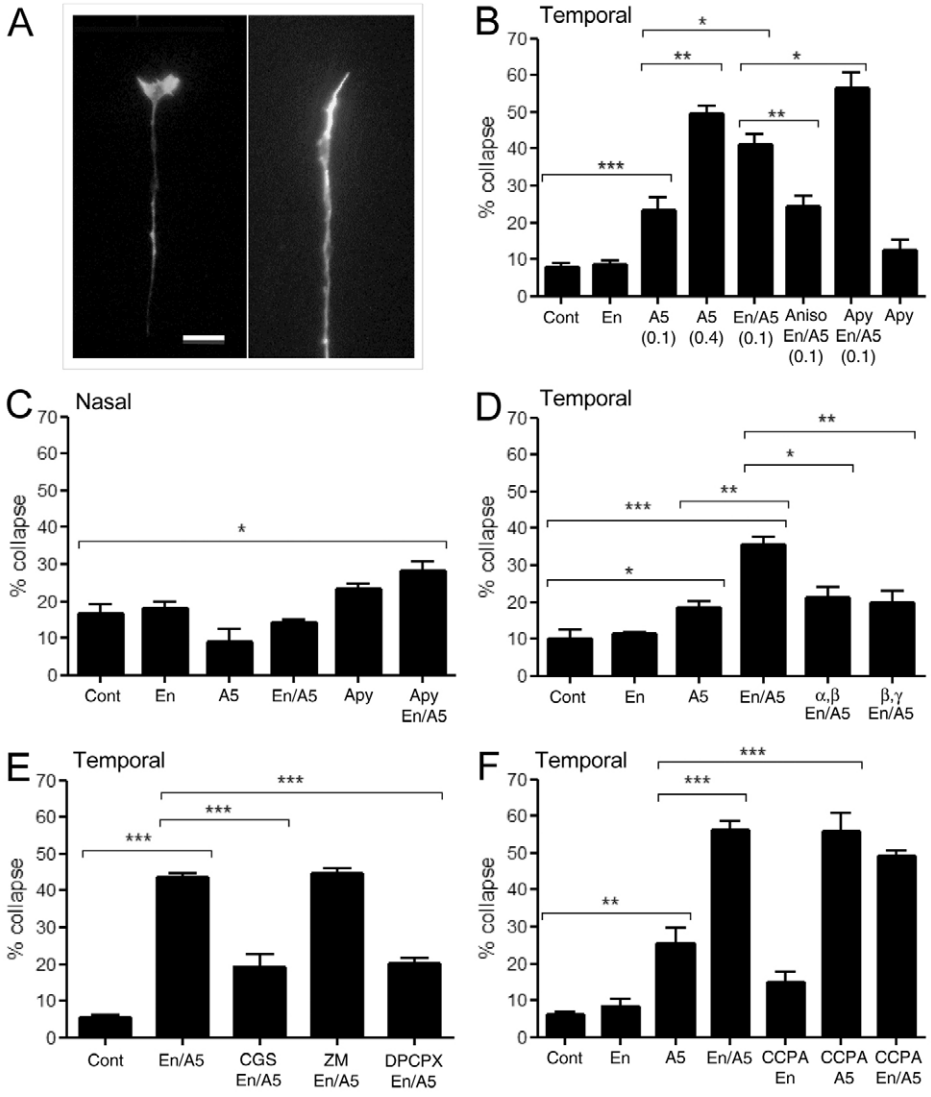

Fig. 4. Engrailed potentiates Ephrin-induced collapse through A1R. (**A**) Normal chick retinal ganglion cell (RGC) growth cone (left) and after collapse (right). (**B-F**) Quantification of temporal and nasal growth cone collapse under various conditions. Ephrin A5 was used at 0.1 μg/ml. A minimum of 235 growth cones was counted per condition and each graph represents an independent experiment. Statistical analyses were performed using one-way ANOVA ($P<0.001$) and two-tailed Student's *t*-test (*$P<0.05$, **$P<0.01$, ***$P<0.001$). En, Engrailed; A5, ephrin A5; Apy, apyrase; aniso, anisomycin; α,β, α,β-methylene-ATP; β,γ, β,γ-methylene-ATP; CGS, CGS15943; ZM, ZM 241385. Scale bar: 18 μm.

repelled by the stripes of posterior tectal membranes and preferentially grow along the interstripes (Fig. 6A). When treated with the A1R antagonist DPCPX, many axons grow across posterior membrane stripes (Fig. 6B). Quantitative analysis shows that, in the control condition, only ~27% of the fluorescence of the RGC axons was in the stripe region, with 73% in the unlabelled anterior membrane stripe region demonstrating a significant repulsion by posterior membranes. In the presence of 100 nM DPCPX, 50% of the temporal RGC axon fluorescence was present on the posterior membrane stripes. This level of growth on the posterior membrane stripes was indistinguishable from that expected if growth were random (i.e. 52%, dashed line in Fig. 6C) and it was significantly different from the DMSO control condition. These results show that blocking A1R reduces the sensitivity of temporal RGC axons to repulsive guidance cues.

A model of retina-to-tectum mapping that includes A1R signalling

We used our model to compare the precision of retina-to-tectum mapping with and without Engrailed/A1R signalling. With Ephrin signalling alone, equation 5 shows that the variability δy_0 of the axonal stopping position is inversely proportional to the slope β_e of the ephrin A5 gradient in the tectum. As a consequence, a shallow ephrin A5 gradient leads to a large variability in the stop position, which does not allow for precise mapping. By contrast, with Engrailed feedback, equation 8 shows that the variability can be greatly reduced, leading to much more precise mapping. In Fig. 7A we display the stopping position y_0 and the variability δy_0 for two temporal axons originating from x_0=0.9 and x_0=0.7 with ephrin A5 signalling alone, and in Fig. 7B we show how Engrailed signalling reduces the variance without changing the mapping (the plots are obtained with $\beta_E=\beta_e=\beta_A=\beta_{eg}=1$ and $\delta T/T=\delta\tilde{T}/\tilde{T}=0.1$).

We conclude that a non-linear amplification mechanism between the Engrailed and ephrin A5 signalling pathways significantly increases the mapping precision even if the ephrin A5 and Engrailed gradients are shallow. By contrast, in the absence of Engrailed feedback, a high mapping precision would require a much steeper ephrin A5 gradient.

We did not consider the role of spontaneous activity in the precision of the retinotopic mapping. The mechanism discussed here provides an initial mapping that is further refined by spontaneous activity. However, as suggested by experimental results (Bevins et al., 2011; Reber et al., 2004), the precision of this initial mapping is very important because spontaneous activity cannot correct misaligned RGC axons if the variance of this initial mapping is too large.

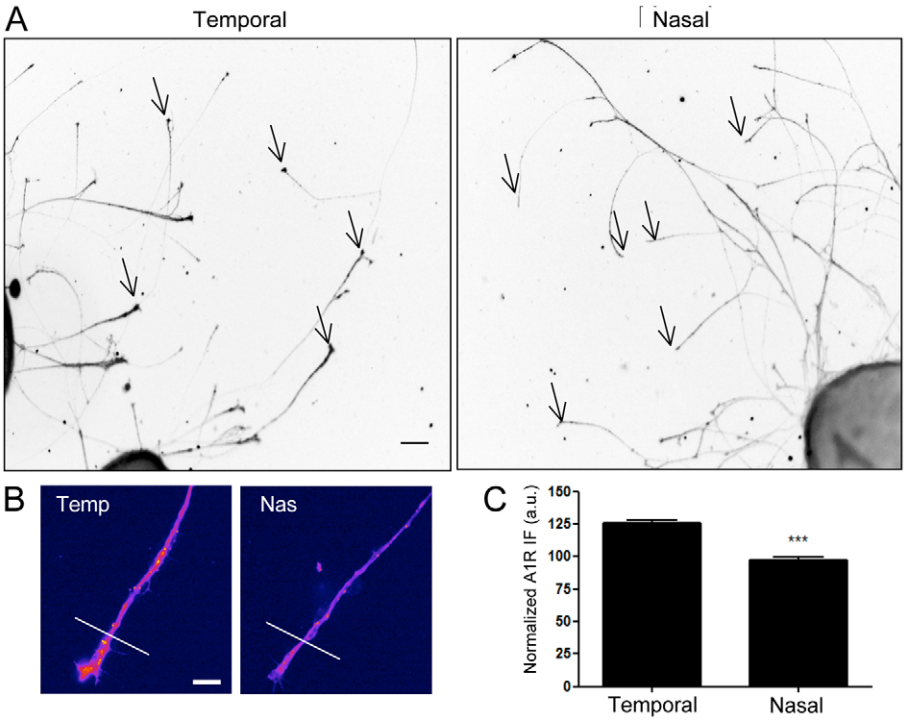

Fig. 5. Local concentrations of A1R immunofluorescence in temporal and nasal RGC growth cones. (**A**) A1R immunostaining of temporal and nasal retinal explants. Arrows indicate growth cones. (**B**) Higher magnification of temporal and nasal growth cones. Images were obtained under identical conditions and have the same background. The white line indicates the limit of the growth cone enlargement. (**C**) Analysis of fluorescence levels after normalisation to growth cone size shows significantly higher concentrations of A1R in temporal than nasal growth cones. Mean ± s.e.m. ***P<0.001, Student's t-test. Scale bars: 100 μm in A; 12 μm in B.

Engrailed signalling through A1R would also take place in the absence of an A1R gradient, raising the issue of temporal/nasal differences in A1R growth cone expression. With graded A1R expression, the onset of ephrin A5 amplification is graded (see Fig. 7B) and temporal axons reach the amplification position at a more anterior position than nasal axons, allowing the latter axons to reach more posterior positions. Without the A1R gradient, the Engrailed signal $S_{eg}(y)$ depends only on the tectal position y, and all axons experience the same Engrailed signal at a given position y. In this case, the contributions of the gradients of ephrin A5 and of EphA2 to retinotopic precision are amplified equally in all axons regardless of their retinal origin. Engrailed increases precision, but without a gradient of A1R expression the projection map is compressed (Fig. 7C).

DISCUSSION

The ability of homeoproteins to transfer between cells suggests that, in addition to their cell-autonomous activity as transcription and translation regulators (Topisirovic and Borden, 2005), they also have direct non-cell-autonomous signalling activities (Brunet et al., 2007; Joliot and Prochiantz, 2004; Prochiantz and Joliot, 2003). The non-cell-autonomous hypothesis has been verified in vivo for the homeoproteins Pax6, Otx2 and Engrailed (Layalle et al., 2011; Lesaffre et al., 2007; Sugiyama et al., 2008). In vitro studies have shown that growth cone guidance activity by internalised Engrailed is not transcription dependent but requires local protein translation (Brunet et al., 2005). This translation-dependent mode of action was further demonstrated using the collapse assay, in which protein synthesis inhibitors,

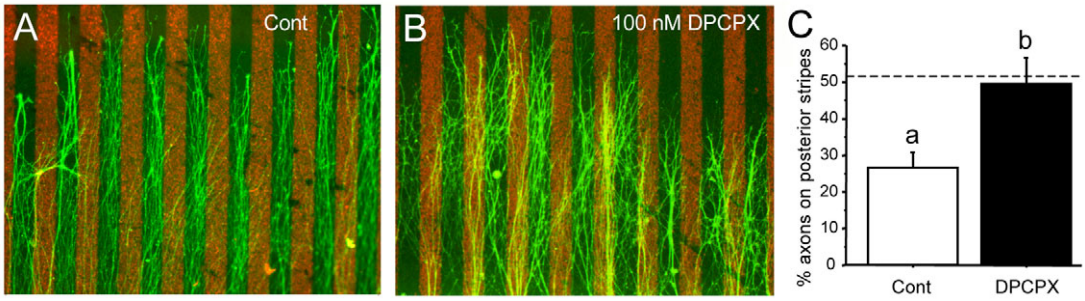

Fig. 6. The A1R antagonist DPCPX interferes with RGC axon guidance. (**A**,**B**) Temporal chick retinal strips were cultured on alternate stripes of posterior (red), which in the experiment covers 52% of the Nuclepore filter, and anterior tectal membrane (unlabelled). Control (DMSO) (A) or DPCPX (B) was added 12 and 24 hours after plating. Forty-eight hours later, explants were fixed and RGC axons pre-labelled with DiAsp were visualised. In control conditions, temporal axons (DiAsp, green) grow preferentially on the anterior membrane stripes (A) and this preference is lost upon A1R inhibition (B). (**C**) Quantification of the growth on posterior membranes. In control conditions, only 27% of the axons grew on posterior membranes (a, P<0.005, one-sample t-test; H_0 (the null hypothesis) =52%). After DPCPX treatment, 50% of the temporal axon fluorescent signal was observed on the posterior membrane stripes (P>0.86, one-sample t-test; H_0=52). DPCPX (n=6) significantly increased temporal axon growth on the posterior membrane stripes compared with vehicle-treated (n=5) explants (b, P<0.05, unpaired t-test). Dashed line, expected level of growth on the posterior membrane stripes if growth were random. Mean ± s.e.m.

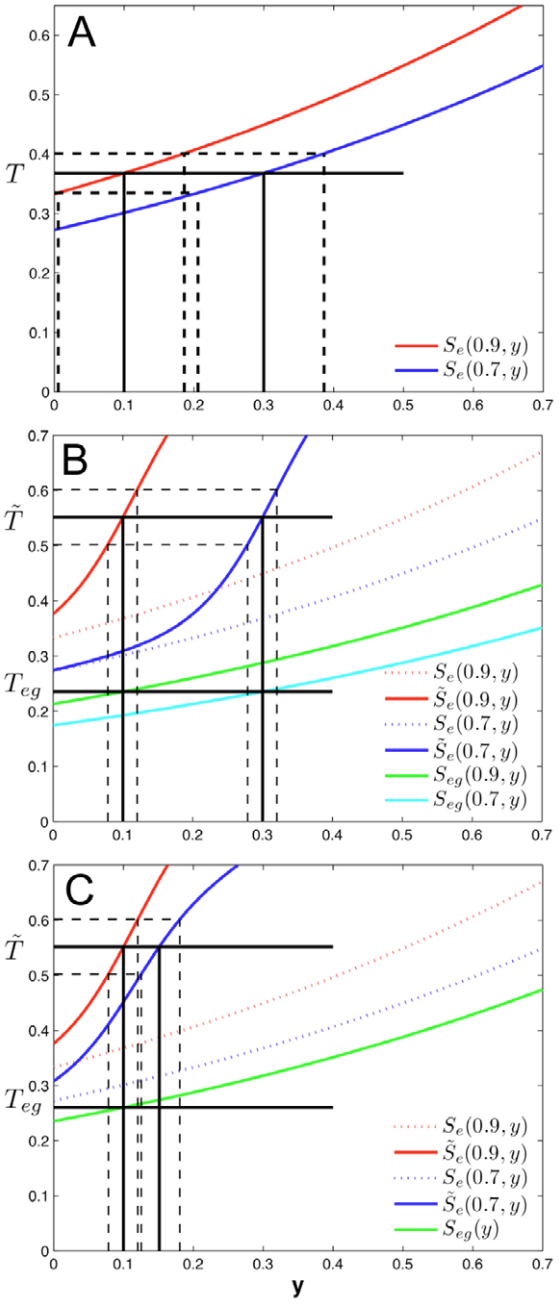

Fig. 7. Engrailed feedback of ephrin A5 signalling increases the axonal stop precision. The plots show the stop position and the corresponding error for two temporal axons from retinal position x_0=0.9 and x_0=0.7 without and with engrailed synergy. The plots are obtained with $\Lambda(s)$ as displayed in supplementary material Fig. S1 and with $\beta_E=\beta_e=\beta_A=\beta_{eg}=1$ and $\delta T/T=\delta\tilde{T}/\tilde{T}=0.1$. (**A**) Ephrin A5 signalling alone leads to a large variance in the stop position (y_0=0.1 for x_0=0.9, and y_0=0.3 for x_0=0.7). (**B**) Engrailed synergy reduces the variance and leads to a more precise mapping. (**C**) Same scenario as in B, but without the A1R gradient. In this case, the Engrailed signal $S_{eg}(y)$ depends only on the retinal position y due to the Engrailed gradient, and all axons experience the same signal. For the figure, we assumed that $S_{eg}(y)$ is given by $S_{eg}(0.9,y)$ as displayed in B, which leads to the same mapping for the axon from x_0=0.9 as in B. The axon from x_0=0.7 experiences the engrailed signal T_{eg} at a more anterior position compared with B, which also leads to a more anterior stop position. The mapping in C is therefore compressed compared with the mappings in A and B.

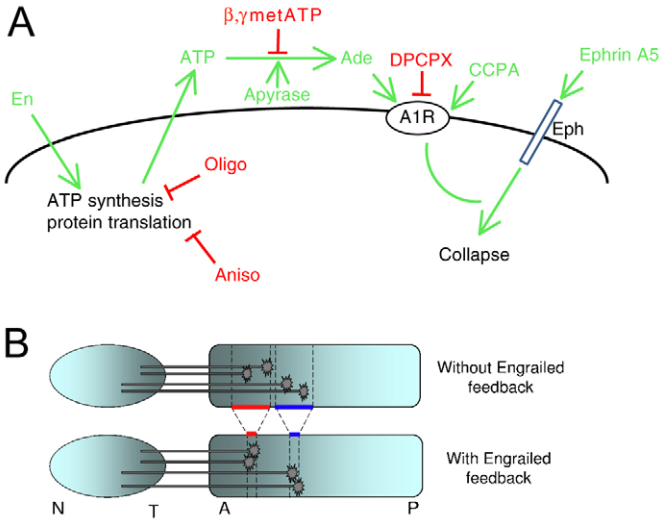

Fig. 8. Summary of results showing that Engrailed feedback of Ephrin signalling increases the axonal stop precision. (**A**) The non-cell-autonomous signalling pathway of Engrailed in growth cones. Green, Engrailed pathway for growth cone collapse. Red, inhibition of growth cone collapse. (**B**) Schematic showing the initial position of the axons in the retina and the variance of their stop position in the tectum without and with Engrailed feedback as explained by the model and described in Fig. 7A,B. N, nasal; T, temporal; A, anterior; P, posterior.

but not inhibitors of transcription, abrogate the Engrailed-associated sensitization of temporal cones to subthreshold ephrin A5 concentrations (Wizenmann et al., 2009).

The present study has investigated the Engrailed signalling pathway (as summarised in Fig. 8) and used a simplified in vitro model to establish that Engrailed sensitizes temporal growth cones to ephrin A5 signalling. This sensitization requires Engrailed-controlled and protein synthesis-dependent ATP synthesis and ATP secretion. Although this is the first time that ATP secretion from the growth cone has been observed, it is important to note that a similar timecourse for ATP secretion, using a different approach, has recently been reported from the axon trunk (Fields and Ni, 2010). Growth cone secreted ATP is then degraded into adenosine, which signals back to the growth cone through A1R. Accordingly, an A1R agonist enhances ephrin A5 signalling in the absence of Engrailed. The differential density of A1R in growth cones (low nasal and high temporal) might explain, in part, why nasal axons are less sensitive to the combined addition of Engrailed and ephrin A5.

A first observation is that this interaction only takes place in vitro at subthreshold ephrin A5 concentrations. Indeed, raising ephrin A5 concentrations to 0.4 μg/ml provokes collapse in the absence of Engrailed or adenosine ‘co-factors’. One can propose that these subthreshold concentrations are physiological because the neutralization of Engrailed with a blocking agent on membrane stripes or in vivo (where ephrin A5 is present at normal – but unknown – concentrations) leads to temporal RGC guidance errors (Wizenmann et al., 2009).

Our results show that Engrailed stimulates rapid ATP neosynthesis (1-5 minutes), and that the increase in ATP outside the growth cone as early as 1 minute (average 2 minutes 43 seconds) is protein translation dependent. The inhibition of ATP synthesis by oligomycin demonstrates that secreted ATP is newly synthesized following Engrailed entry. The idea that homeoproteins regulate

translation has been proposed before (Topisirovic and Borden, 2005) and a role of Engrailed-regulated protein translation in axon guidance has already been demonstrated (Brunet et al., 2005). In the present case, Engrailed might act at different levels, possibly regulating the translation of peri-mitochondrial mRNAs, in particular those encoding complex I factors, as we showed in ventral mouse midbrain (Alvarez-Fischer et al., 2011), but also that of proteins involved in ATP release or growth cone physiology and morphology. Future studies will be necessary to clarify this point.

In any case, the entire ATP neosynthesis process takes place within a few minutes. Given that protein synthesis in vertebrates occurs at a rate of six to nine amino acids per second, 1 minute would be sufficient to synthesize a protein of 360 amino acids, making the rapid ATP synthesis and release that we observe conceivable.

Classical signalling molecules, such as Ephrins, signal through their cognate receptors. Our data show that, at least in this experimental model, Engrailed, which to our knowledge has no classical receptor, signals via adenosine and A1R. Homeoproteins are ancestral proteins expressed in unicellular organisms (Derelle et al., 2007) and homeoprotein signalling is conserved in plants and animals (Ruiz-Medrano et al., 2004; Tassetto et al., 2005), suggesting that homeoproteins were probably operating in the first multicellular organisms. Therefore, it is conceivable that the regulation of intracellular ATP concentration by homeoprotein transfer, with local metabolic and regulatory effects (i.e. activation of cytoskeleton regulatory factors), might have provided a primitive mode of signalling and that it is only later in the course of evolution that ATP secretion and purinergic receptor activation have been incorporated in the loop. Indeed, ATP is extremely ubiquitous and the chemotactic properties of purinergic compounds have been described in many systems (Benowitz et al., 1998; Chen et al., 2006; Davalos et al., 2005; Kronlage et al., 2010; Orr et al., 2009), including growth cone guidance (Fu et al., 1997; Grau et al., 2008).

Ephrin A5 and Engrailed are present in low-anterior, high-posterior gradients in the chick optic tectum (Drescher et al., 1997; Wizenmann et al., 2009), whereas EphA2 and A1R show high-temporal, low-nasal expression in RGC growth cones. Our data reveal that Engrailed signalling via A1R sensitizes temporal growth cones to low concentrations of ephrin A5 (0.1 μg/ml) and strengthen previous observations of A1R involvement in retinotectal patterning (Tavares Gomes et al., 2009). Based on this finding, we developed a computational model showing how a non-linear interaction between Engrailed and ephrin A5 signalling pathways increases the precision of growth cone navigation. Our model explains how Engrailed signalling through A1R increases not only the sensitivity of temporal cones to ephrin A5 but also the precision of their navigation, thus illustrating how different signalling pathways can cooperate to create precise and robust patterns. Furthermore, the model predicts, and the experimental data suggest, that at low (and possibly physiological) ephrin A5 concentration the two pathways are necessary (and neither alone sufficient) to establish the precision observed in vivo.

In conclusion, this simple novel signalling mechanism based on homeoprotein non-cell-autonomous transcription is in fact much more complex than anticipated. Not only does it involve local translation, but it also cooperates with classical signalling – in the present case, A1R and the Ephrin/Eph pathways.

Acknowledgements
We thank Ouardane Jouannot for help in preliminary ATP imaging experiments; Ulrike Kohler for excellent technical assistance; François Darchen for support; and Paola Bovolenta for critical reading of the paper.

Funding
This work was supported by grants from the Agence Nationale de la Recherche [ANR-08-BLAN-0162-01] (Borderline); Global Research Laboratory (South Korea) Program; and the European Community [FP7 222999 MdANEURODEV] and partially supported by an ERC-SG.

Competing interests statement
The authors declare no competing financial interests.

Author contributions
O.S., R.L.J. and K.L.M. carried out growth cone preparation, metabolic labelling and collapse assay experiments; R.L.J. and C.B. carried out proteomic analyses; O.S. carried out ATP imaging experiments; A.W. carried out stripe assays; J.R. and D.H. developed the computational model and carried out computational analyses; F.C. designed, constructed and produced the Engrailed mutant and performed Ndufs3 western blotting; and O.S., A.P. and K.L.M. designed experiments, analysed data and wrote the paper.

Supplementary material
Supplementary material available online at
http://dev.biologists.org/lookup/suppl/doi:10.1242/dev.063875/-/DC1

References

Alvarez-Fischer, D., Fuchs, J., Castagner, F., Stettler, O., Massiani-Beaudoin, O., Moya, K. L., Bouillot, C., Oertel, W. H., Lombes, A., Faigle, W. et al. (2011). Engrailed protects mouse midbrain dopaminergic neurons against mitochondrial complex I insults. *Nat. Neurosci.* **14**, 1260-1266.
Baier, H. and Bonhoeffer, F. (1992). Axon guidance by gradients of a target-derived component. *Science* **255**, 472-475.
Benowitz, L. I., Jing, Y., Tabibiazar, R., Jo, S. A., Petrausch, B., Stuermer, C. A., Rosenberg, P. A. and Irwin, N. (1998). Axon outgrowth is regulated by an intracellular purine-sensitive mechanism in retinal ganglion cells. *J. Biol. Chem.* **273**, 29626-29634.
Bevins, N., Lemke, G. and Reber, M. (2011). Genetic dissection of EphA receptor signaling dynamics during retinotopic mapping. *J. Neurosci.* **31**, 10302-10310.
Brown, A., Yates, P. A., Burrola, P., Ortuno, D., Vaidya, A., Jessell, T. M., Pfaff, S. L., O'Leary, D. D. and Lemke, G. (2000). Topographic mapping from the retina to the midbrain is controlled by relative but not absolute levels of EphA receptor signaling. *Cell* **102**, 77-88.
Brunet, I., Weinl, C., Piper, M., Trembleau, A., Volovitch, M., Harris, W., Prochiantz, A. and Holt, C. (2005). The transcription factor Engrailed-2 guides retinal axons. *Nature* **438**, 94-98.
Brunet, I., Di Nardo, A. A., Sonnier, L., Beurdeley, M. and Prochiantz, A. (2007). The topological role of homeoproteins in the developing central nervous system. *Trends Neurosci.* **30**, 260-267.
Burnstock, G. (2006). Purinergic signalling-an overview. *Novartis Found. Symp.* **276**, 26-48; discussion 48-57, 275-281.
Burnstock, G. (2008). Purinergic signalling and disorders of the central nervous system. *Nat. Rev. Drug Discov.* **7**, 575-590.
Chen, Y., Corriden, R., Inoue, Y., Yip, L., Hashiguchi, N., Zinkernagel, A., Nizet, V., Insel, P. A. and Junger, W. G. (2006). ATP release guides neutrophil chemotaxis via P2Y2 and A3 receptors. *Science* **314**, 1792-1795.
Chihara, T., Luginbuhl, D. and Luo, L. (2007). Cytoplasmic and mitochondrial protein translation in axonal and dendritic terminal arborization. *Nat. Neurosci.* **10**, 828-837.
Corriden, R., Insel, P. A. and Junger, W. G. (2007). A novel method using fluorescence microscopy for real-time assessment of ATP release from individual cells. *Am. J. Physiol. Cell Physiol.* **293**, C1420- C1425.
Davalos, D., Grutzendler, J., Yang, G., Kim, J. V., Zuo, Y., Jung, S., Littman, D. R., Dustin, M. L. and Gan, W. B. (2005). ATP mediates rapid microglial response to local brain injury in vivo. *Nat. Neurosci.* **8**, 752-758.
Derelle, R., Lopez, P., Le Guyader, H. and Manuel, M. (2007). Homeodomain proteins belong to the ancestral molecular toolkit of eukaryotes. *Evol. Dev.* **9**, 212-219.
Drescher, U., Bonhoeffer, F. and Muller, B. K. (1997). The Eph family in retinal axon guidance. *Curr. Opin. Neurobiol.* **7**, 75-80.
Fields, R. D. and Ni, Y. (2010). Nonsynaptic communication through ATP release from volume-activated anion channels in axons. *Sci. Signal.* **3**, ra73.
Flanagan, J. G. (2006). Neural map specification by gradients. *Curr. Opin. Neurobiol.* **16**, 59-66.
Friedman, G. C. and O'Leary, D. D. (1996). Retroviral misexpression of engrailed genes in the chick optic tectum perturbs the topographic targeting of retinal axons. *J. Neurosci.* **16**, 5498-5509.
Fu, W. M., Tang, Y. B. and Lee, K. F. (1997). Turning of nerve growth cones induced by the activation of protein kinase C. *NeuroReport* **8**, 2005-2009.
Goodhill, G. J. and Baier, H. (1998). Axon guidance: stretching gradients to the limit. *Neural Comput.* **10**, 521-527.

Gordon-Weeks, P. R. and Lockerbie, R. O. (1984). Isolation and partial characterisation of neuronal growth cones from neonatal rat forebrain. *Neuroscience* **13**, 119-136.
Grau, B., Eilert, J. C., Munck, S. and Harz, H. (2008). Adenosine induces growth-cone turning of sensory neurons. *Purinergic Signal.* **4**, 357-364.
Holcman, D., Kasatkin, V. and Prochiantz, A. (2007). Modeling homeoprotein intercellular transfer unveils a parsimonious mechanism for gradient and boundary formation in early brain development. *J. Theor. Biol.* **249**, 503-517.
Itasaki, N. and Nakamura, H. (1996). A role for gradient en expression in positional specification on the optic tectum. *Neuron* **16**, 55-62.
Joliot, A. and Prochiantz, A. (2004). Transduction peptides: from technology to physiology. *Nat. Cell Biol.* **6**, 189-196.
Kettlun, A. M., Uribe, L., Calvo, V., Silva, S., Rivera, J., Mancilla, M., Valenzuela, M. A. and Traverso-Cori, A. (1982). Properties of two apyrarses from *Solanum tuberosum*. *Phytochemistry* **21**, 551-558.
Kronlage, M., Song, J., Sorokin, L., Isfort, K., Schwerdtle, T., Leipziger, J., Robaye, B., Conley, P. B., Kim, H. C., Sargin, S. et al. (2010). Autocrine purinergic receptor signaling is essential for macrophage chemotaxis. *Sci. Signal.* **3**, ra55.
Kvanta, A., Seregard, S., Sejersen, S., Kull, B. and Fredholm, B. B. (1997). Localization of adenosine receptor messenger RNAs in the rat eye. *Exp. Eye Res.* **65**, 595-602.
Layalle, S., Volovitch, M., Mugat, B., Bonneaud, N., Parmentier, M. L., Prochiantz, A., Joliot, A. and Maschat, F. (2011). Engrailed homeoprotein acts as a signaling molecule in the developing fly. *Development* **138**, 2315-2323.
Lesaffre, B., Joliot, A., Prochiantz, A. and Volovitch, M. (2007). Direct non-cell autonomous Pax6 activity regulates eye development in the zebrafish. *Neural Develop.* **2**, 2.
Logan, C., Wizenmann, A., Drescher, U., Monschau, B., Bonhoeffer, F. and Lumsden, A. (1996). Rostral optic tectum acquires caudal characteristics following ectopic engrailed expression. *Curr. Biol.* **6**, 1006-1014.
Matsuoka, I. and Ohkubo, S. (2004). ATP- and adenosine-mediated signaling in the central nervous system: adenosine receptor activation by ATP through rapid and localized generation of adenosine by ecto-nucleotidases. *J. Pharmacol. Sci.* **94**, 95-99.
Ongini, E., Dionisotti, S., Gessi, S., Irenius, E. and Fredholm, B. B. (1999). Comparison of CGS 15943, ZM 241385 and SCH 58261 as antagonists at human adenosine receptors. *Naunyn Schmiedebergs Arch. Pharmacol.* **359**, 7-10.
Orr, A. G., Orr, A. L., Li, X. J., Gross, R. E. and Traynelis, S. F. (2009). Adenosine A(2A) receptor mediates microglial process retraction. *Nat. Neurosci.* **12**, 872-878.
Prochiantz, A. and Joliot, A. (2003). Can transcription factors function as cell-cell signalling molecules? *Nat. Rev. Mol. Cell Biol.* **4**, 814-819.
Reber, M. and Lemke, G. (2005). Retinotectal mapping: new insights from molecular genetics. *Annu. Rev. Cell Dev. Biol.* **21**, 551-580.
Reber, M., Burrola, P. and Lemke, G. (2004). A relative signalling model for the formation of a topographic neural map. *Nature* **431**, 8478-8453.
Ruiz-Medrano, R., Xoconostle-Cazares, B. and Kragler, F. (2004). The plasmodesmatal transport pathway for homeotic proteins, silencing signals and viruses. *Curr. Opin. Plant Biol.* **7**, 641-650.
Scicolone, G., Ortalli, A. L. and Carri, N. G. (2009). Key roles of Ephs and ephrins in retinotectal topographic map formation. *Brain Res. Bull.* **79**, 227-247.
Sugiyama, S., Di Nardo, A. A., Aizawa, S., Matsuo, I., Volovitch, M., Prochiantz, A. and Hensch, T. K. (2008). Experience-dependent transfer of Otx2 homeoprotein into the visual cortex activates postnatal plasticity. *Cell* **134**, 508-520.
Talha, S. and Harel, L. (1986). Anisomycin and cycloheximide, like growth factors, stimulate rapidly ATP turnover in 3T3 cells. *Cell Biol. Int. Rep.* **10**, 249-255.
Tassetto, M., Maizel, A., Osorio, J. and Joliot, A. (2005). Plant and animal homeodomains use convergent mechanisms for intercellular transfer. *EMBO Rep.* **6**, 885-890.
Tavares Gomes, A. L., Maia, F. B., Oliveira-Silva, P., Marques Ventura, A. L., Paes-De-Carvalho, R., Serfaty, C. A. and Campello-Costa, P. (2009). Purinergic modulation in the development of the rat uncrossed retinotectal pathway. *Neuroscience* **163**, 1061-1068.
Topisirovic, I. and Borden, K. L. (2005). Homeodomain proteins and eukaryotic translation initiation factor 4E (eIF4E): an unexpected relationship. *Histol. Histopathol.* **20**, 1275-1284.
Wizenmann, A., Brunet, I., Lam, J. S. Y., Sonnier, L., Beurdeley, M., Zarbalis, K., Weisenhorn-Vogt, D., Weiln, C., Dwivedy, A., Joliot, A. et al. (2009). Extracellular Engrailed participates in the topographic guidance of retinal axons in vivo. *Neuron* **64**, 355-366.
Yates, P. A., Roskies, A. L., McLaughlin, T. and O'Leary, D. D. (2001). Topographic-specific axon branching controlled by ephrin-As is the critical event in retinotectal map development. *J. Neurosci.* **21**, 8548-8563.
Yates, P. A., Holub, A. D., McLaughlin, T., Sejnowski, T. J. and O'Leary, D. D. (2004). Computational modeling of retinotopic map development to define contributions of EphA-ephrinA gradients, axon-axon interactions, and patterned activity. *J. Neurobiol.* **59**, 95-113.